Published in final edited form as:
Biochemistry. 2007 August 21; 46(33): 9355–9365.

Unusual Structural Features of Hydantoin Lesions Translate into Efficient Recognition by *Escherichia coli* Fpg†

Nirmala Krishnamurthy[ℵ], **James G. Muller**[ℵ], **Cynthia J. Burrows**[ℵ], and **Sheila S. David**[*,+]
Department of Chemistry, University of California, Davis, One Shields Avenue, Davis, CA, 95616 and Department of Chemistry, University of Utah, 315 South, 1400 East, Salt Lake City, Utah 84112

Abstract

Oxidation of guanine (G) and 8-oxoguanine (OG) with a wide variety of oxidants yields the hydantoin lesions, guanidinohydantoin (Gh) and spiroiminodihydantoin (Sp). These two lesions have garnered much recent attention due to their unusual structures and high mutagenic potential. We have previously shown that duplexes containing Gh and Sp are substrates for the base excision repair glycosylase *Escherichia coli* Fpg (EcFpg). In order to evaluate the recognition features of these unusual lesions, binding and footprinting experiments were performed using a glycosylase inactive variant, E3Q EcFpg and 30 bp duplexes containing the embedded lesions. Surprisingly, E3Q EcFpg was found to bind significantly more tightly (~1000-fold) to duplexes containing Gh or Sp over the corresponding duplexes containing OG. This may be a consequence of the helixdestabilizing nature of the hydantoin lesions that facilitates their recognition within duplex DNA. Though DNA binding affinities of E3Q EcFpg with Gh- and Sp- containing duplexes were found to be similar to each other, hydroxyl radical footprinting using methidium-propyl-EDTA (MPE)- Fe(II) revealed subtle differences between binding of E3Q EcFpg with the two lesions. Most notably, in the presence of E3Q EcFpg, the Sp nucleotide (nt) is hyperreactive towards cleavage by MPE-Fe(II) generated hydroxyl radicals suggestive of the formation of an intercalation site for the MPE-Fe(II) reagent at the Sp nt. Interestingly, increasing the duplex length from 18 to 30 bp enhanced the excision efficiency of Gh and Sp paired with C, G or T by EcFpg such that these substrates are processed as efficiently as the signature substrate lesion OG. Moreover, the base removal activity with these two lesions was *more* efficient than removal of OG when in a base pairing context opposite A. The high affinity and efficient activity of EcFpg towards the hydantoin lesions suggests that EcFpg mediates repair of the lesions *in vivo*. Notably, the facile activity of EcFpg towards Gh and Sp in base pairing contexts with G and A, which are likely to be present after DNA replication, would be detrimental and enhance mutagenesis.

Reactive oxygen species (ROS),[1] such as superoxide, hydrogen peroxide, and hydroxyl radicals, are formed as byproducts of cellular metabolism or indirectly via external sources such as ionizing radiation (1,2). The presence of ROS can lead to various types of DNA damage

†This work was supported by a grant from the National Cancer Institute of the National Institutes of Health (CA90689)

*Corresponding Author: SSD: telephone: (530)-752-4830; fax: (530)-752-8995, Email address: david@chem.ucdavis.edu.
+Department of Chemistry, University of California, Davis
ℵDepartment of Chemistry, University of Utah

[2]Most glycosylases have a high affinity for the product, and in many cases higher than for the substrate. It should also be noted that many of the previous reports measured the K_d values using DNA concentrations that were close to K_d (i.e. too high), and this may also contribute to inaccurate determinations of K_d.

[1]Abbreviations: *Bacillus stearothermophilus* Fpg, BsFpg; BER, base excision repair; bp, base-pair; BSA, bovine serum albumin; DTT, dithiothreiotol; *Escherichia coli* Fpg, EcFpg; EDTA, ethylenediamine-tetraacetic acid; 2,6-diamino-4-hydroxy-5-formamidopyrimidine (FapydG), Fpg, formamidopyrimidine glycosylase or MutM; Gh, guanidinohydantoin; human OG glycosylase 1 (hOGG1); IPTG, isopropyl β-D-thiogalactoside; nt, nucleotide; OG, 7,8-dihydro-8-oxoguanine; MPE, methidium propyl EDTA; PAGE, polyacrylamide gel electrophoresis; ROS, reactive oxygen species; Sp, spiroiminodihydantoin; TBE, trisborate-EDTA; THF, tetrahydrofuran nucleotide; Tris, tris(hydroxymethyl)aminomethane

including strand breaks, protein-DNA cross-links, abasic sites, and base lesions, which are potentially mutagenic and toxic to the cell (1,3–5). Fortunately, the integrity of DNA is preserved by a variety of DNA repair pathways (6–9). Indeed, defective DNA repair enzymes have been implicated in carcinogenesis, aging, and neurological disorders (10–13)

Much of the focus of oxidative base damage has been on the oxidation product of guanosine, 7, 8-dihydro-8-oxo-2′-deoxyguanosine (OG), as the key biomarker of cellular oxidation (4, 14,15). However, a wide variety of oxidized guanine lesions have been identified, either resulting from further oxidation of OG or from direct oxidation of G (16). Of these further oxidized products, the hydantoin lesions, spiroiminodihydantoin (Sp) and guanidinohydantoin (Gh) (17,18) (Figure 1A) have interesting structural properties, and have been identified as products in isolated DNA from oxidation of G and OG with a variety of oxidants, including singlet oxygen (19,20), type I photochemistry involving superoxide (21,22), high-valent chromium compounds (23,24) and peroxynitrite (25–27). The ability to form Sp and Gh under a variety of conditions is highly suggestive of their formation within cells. Indeed, recently, Sp was detected by ESI-MS in repair-deficient *E. coli* that had been treated with chromate (28).

The hydantoin lesions have also been demonstrated to be highly mutagenic through both *in vitro* and *in vivo* studies. In single nucleotide insertion and primer extension experiments using *E. coli* Klenow fragment of DNA polymerase exonuclease (−) (KF exo$^-$), dAMP and dGMP are inserted opposite these oxidized lesions (29,30). The response of DNA polymerases to OG is distinctly different with misinsertion of dAMP as well as correct insertion of dCMP to differing extents depending on the polymerase (31). However, in cellular experiments, OG is only mildly mutagenic mediating G:C to T:A transversion mutations (~10%) (32,33). In contrast, in *E. coli* based mutagenesis assays with single-stranded lesion containing viral DNA, Gh and Sp are potently mutagenic causing both G→ T and G→ C transversion mutations (34,35).

An important feature that influences the mutagenic potential of a given lesion is the efficiency of its repair, and the sensitivity of the repair enzymes to the correct base pairing context. The relatively low mutation frequency of OG, in both *E. coli* and mammalian cells, is due to efficient repair (36,37). The *E. coli* enzyme MutT hydrolyzes dOGTP to dOGMP to prevent its misincorporation in the replicating DNA (38). The prevention of mutations associated with OG formed within duplex DNA in *E. coli* requires two base excision repair (BER) glycosylases MutM and MutY (7,13,39–43). *E. coli* MutM, also known as formamidopyrimidine glycosylase (EcFpg), removes OG from OG:C mispairs in the DNA duplex. Other enzymes of the BER pathway then act sequentially to restore the appropriate G:C bp. Any OG:A bps formed during replication are intercepted by MutY which removes the inappropriately inserted adenine residues, thereby allowing recreation of an appropriate OG:C substrate for EcFpg. Functionally similar BER glycosylases are also present in other organisms (9,40).

Structural studies of E3Q *Bacillus stearothermophilus* Fpg (BsFpg), a glycosylase inactive variant, bound to an OG:C substrate have illustrated features that allow for discrimination of OG from G (Figure 1B) (44). In addition to OG, Fpg has been shown to catalyze the removal of a variety of damaged bases including ring-opened forms of purines such as 2,6-diamino-4-hydroxy-5-formamidopyrimidine (FapyG) and 4,6-diamino-5-formamidopyrimidine (FapyA), oxidized pyrimidines such as 5-hydroxycytosine, 5-hydroxyuracil, and 5,6-dihydroxy-5,6-dihydrothymine (40). Previous work in our laboratory has shown that the hydantoin lesions, Gh and Sp are also substrates for EcFpg (45), consistent with the retention of “OG-like” features in these lesions (Figure 1B). Gh and Sp lesions are also removed by endonuclease VIII (Nei) (46) and its mammalian counterparts, mNEIL1 and mNEIL2 (47).

Surprisingly, Gh and Sp are not substrates for human OG glycosylase, hOGG1, though they are substrates for the homologous yeast OG glycosylases, yOGG1 and yOGG2 (45).

In order to further elucidate the features of recognition of the hydantoin lesions relative to OG by EcFpg, we analyzed the binding affinities of a glycosylase inactive variant E3Q EcFpg (44) with 30 bp duplexes containing the embedded lesions. These studies reveal that E3Q EcFpg binds several orders of magnitude more tightly to duplexes containing Gh:C and Sp:C bps over the corresponding duplex containing OG:C. In addition, higher affinity of E3Q EcFpg for Gh and Sp duplexes was observed when the lesions are positioned opposite C than G. Further subtleties in the binding properties of E3Q EcFpg to Gh and Sp-containing duplexes opposite both G and C were revealed using methidium-propyl EDTA (MPE)-Fe(II) hydroxyl-radical footprinting experiments. Indeed, the binding of EcFpg to Sp-containing duplexes creates a “hot-spot” for intercalation at the Sp nucleotide. Interestingly, the use of the longer duplex substrates also enhanced the efficiency of Gh and Sp removal compared to the 18 bp duplex. In fact, the rate of Gh and Sp removal opposite C, G and T by EcFpg is similar to that for OG within the longer duplex. However, when paired with A in both duplex lengths, EcFpg removes Gh and Sp more efficiently than OG. This present work provides insight into features of these lesions that may lead to their efficient recognition and removal by EcFpg.

Materials and methods

General materials and instrumentation

7,8-Dihydro-8-oxo-2′-deoxyguanosine phosphoramidite was purchased from Glen Research. DNA oligonucleotides were synthesized according to the manufacturer’s protocol on an Applied Biosystems model 392 DNA/RNA synthesizer. These samples were purified via HPLC on a Beckman Gold Nouveau system with a Protein-Pak DEAE 8HR column. Oligonucleotides used for mutagenesis via PCR were purified using oligonucleotide purification cartridges (OPC) from Perkin-Elmer. PCR was performed on a GeneAmp PCR system 2400 from Perkin-Elmer. Radiolabeling was done using [γ-^{32}P]ATP purchased from GE Health Sciences with T4 polynucleotide kinase which was obtained from New England BioLabs. Labeled oligonucleotides were purified using ProbeQuant G-50 spin columns from GE Health Sciences according to the manufacturer’s protocol. A Milli-Q PF system was used to purify distilled, deionized water that was used to make all the buffers. All buffers were passed through a 0.45 μm filter before use. Storage phosphor autoradiography was performed on a Typhoon 9400 phosphorimager system. Data analysis was performed using ImageQuaNT software (version 5.2a) and the rate constants were determined from fitting of the data with GraFit 5.0. All other chemicals used for these experiments were purchased from Fisher Scientific, VWR, or Sigma.

Cloning of E3Q EcFpg

The “megaprimer”-based mutagenesis method (Stratagene) was used for site-directed mutagenesis according to the manufacturer’s protocol. The necessary codon change that encodes for the mutated enzyme E3Q EcFpg was incorporated into the *fpg* gene using the following primers. E3Q-1, 5′-GGAGATGCTATGCCTCAATTACCCGAAGTTGAAACC-3′; E3Q-2, 5′-GGTTTCAACTTCGGGTAATTGAGGCATAGCATCTCC-3′.

The altered codon for mutagenesis of the appropriate amino acid is underlined. Plasmid DNA was isolated from XL-1 blue *E. coli* cells using a Wizard Plus DNA purification kit (Promega) according to the manufacturer’s protocol. The presence of the correct mutation was confirmed by DNA sequencing provided by the core facility at the University of Utah Medical School, SLC, UT.

Expression and Purification of WT and E3Q EcFpg

WT EcFpg was isolated using JM109 *E. coli* transformed with the pKKFapy2 overexpression plasmid (48). For the E3Q EcFpg, the corresponding pKKFapy2 plasmid containing the altered fpg gene to produce the E3Q EcFpg protein, pKKE3Q, was transformed into competent CC104 *mutm*$^{-}$ cells. Cell growth, induction and purification procedures for EcFpg and E3Q EcFpg were similar to that reported previously (49). The relevant concentrations of EcFpg or E3Q EcFpg were determined using the absorbance at 280 nm and the extinction coefficient (ε_{280} = 3.9×10^4 L mol^{-1} cm^{-1}). The active EcFpg concentration was determined as reported previously (49). An estimation of the amount of E3Q EcFpg protein competent for DNA binding (assuming a 1:1 binding stoichiometry) was determined using the Gh:C-containing 30 bp duplex (49). This indicated only 7% of the sample was able to bind DNA, and therefore all concentrations of E3Q Fpg were corrected using this value.

Substrate DNA preparation

Gh- and Sp- containing nucleotides were synthesized from the original OG-containing nucleotides as previously described (49). The 30-nucleotide (nt) sequence that was used is listed below: d(5′–TGTTCATCATGGGTC**X**TCGG TATATCCCAT–3′) in which X = OG, Gh, Sp, and the complementary strand d(3′–ACAAGTAGTACCCAG**Y**AGCCATATAGGGTA–5′) in which Y = C, A, T or G. For all experiments, 2.5 pmoles of the X-containing strand was radiolabeled on the 5′ end using [γ-^{32}P]-ATP by T4 kinase at 37 °C. Excess [γ-^{32}P]-ATP was removed using a GE Health Sciences Microspin G-50 spin column, according to the manufacturer's protocol. For the glycosylase activity assays, additional nonradioactive X-containing DNA was added to the labeled strand to allow 5% labeled DNA, which was then annealed to the complement (added at 20% excess) by heating to 90 °C for 5 min and allowing to cool overnight in annealing buffer (20 mM Tris-HCl (pH 7.6), 10 mM EDTA, and 150 mM NaCl). For the binding affinity experiments, an equimolar amount of the complement was added to 100% radiolabeled X-containing DNA. The duplex was then annealed as above. For binding experiments, the listed duplex concentrations are upper-limit values based on 100% assumed recovery after purification and labeling. For the footprinting experiments, either the X- containing or the Y-containing strand was radiolabeled according to the protocol for the binding affinity experiments described above.

Glycosylase Assays

Single-turnover experiments, where [Enz] > [DNA], were performed using the 30 bp duplexes to evaluate the glycosylase activity of the enzymes. In each case, the total reaction volume was 60 μL with a final duplex DNA concentration of 20 nM. The duplex was incubated with 150–300 nM active Fpg in an assay buffer (20 mM Tris-HCl, pH 7.6, 10 mM EDTA, 0.1 mg/mL BSA, and 30 mM NaCl) at 37 °C. Aliquots were removed manually at various times (15 s to 60 min) and quenched by the addition of 5 μL of 0.5 N NaOH. This was followed by the addition of 5μL of formamide denaturing dye (80% formamide, 0.025% xylene cyanol, 0.025% bromophenol blue in TBE buffer) and then the aliquots were heated to 90 °C for 2 min and placed on dry ice. The samples were run on a 15% denaturing polyacrylamide gel in 1X TBE at 1600 V for 2 hours. The separation of the 15 nt DNA fragment arising from the product and the 30 nt fragment originating from the substrate was visualized using autoradiography by exposure to a storage phosphor screen overnight. As a control, for several substrates that could be examined manually, parallel reactions of EcFpg with the substrates were quenched with NaOH or with formamide dye alone. Analysis of extent of strand scission based on these experiments provided similar rates of reactions consistent with tight coupling of the glycosylase and lyase functions of EcFpg since the NaOH treatment would have cleaved any intact abasic sites. Control experiments without enzyme also established that the Gh and Sp lesions were

cleaved minimally by the NaOH quenching (< 5%). The extent of background cleavage due to the NaOH quenching was subtracted during quantitation of the storage phosphor autoradiograms.

For reactions under single-turnover experiments in which the glycosylase reaction was too fast to measure manually, a Rapid Quench Flow instrument (RQF-3) from Kintek was used. The reaction buffer and conditions and overall analysis are similar to the manual experiments. However, notably addition of a nonspecific duplex (25 nM) to the EcFpg (400 nM) while in the injection loop was found to be necessary to stabilize the enzyme. This particular ratio of DNA duplex to EcFpg provided optimal stability, without interfering with the reaction with the substrate duplex. Once mixed with the substrate DNA duplex, the final reaction concentrations were: substrate (20 nM), non-specific DNA duplex (12.5 nM) and EcFpg (200 nM). A water bath maintained the reaction temperature at 37 °C, and reactions were allowed to incubate for time points ranging from 0.1 s and 5 min before being quenched with 0.5 M NaOH. In all cases, the values reported are the average of at least three separate determinations, and the error is reported as the standard deviation of the sample set.

Equilibrium Dissociation Constant (Kd) Measurements

Electrophoretic mobility shift assays (EMSA) were performed to determine the K_d values. Reaction volumes contained 10 pM duplex DNA, 20 mM Tris-HCl pH 7.5, 10 mM NaCl, 1 mM EDTA, 1 mM DTT, 10% glycerol, 0.1 mg/mL BSA, and E3Q Fpg concentrations ranging from 2 μM to 10 pM. Samples of the protein-DNA mixture were incubated at 25 °C for 30 min followed by the addition of 6 μL of nondenaturing loading dye (0.25% bromophenol blue, 0.25% xylene cylanol, 30% glycerol in 1X TBE). Bound versus unbound DNA was resolved using electrophoresis on a 8% nondenaturing polyacrylamide gel (29:1 acrylamide/bis) at 4 °C in 0.5X TBE buffer at 120 V for 2 h. Gels were dried and exposed to a storage phosphor screen overnight. K_d values were determined by fitting the data (percent bound substrate versus enzyme concentration) using a one-site binding isotherm (Grafit 5.0).

Methidiumpropyl-EDTA Fe(II) Footprinting experiments

Hydroxyl radical footprinting experiments using methidiumpropyl EDTA Fe(II) [MPE-Fe(II)] were performed following the procedure previously reported by our laboratory (50). Briefly, reactions (10 μL) containing 10 nM 5′-end-labeled duplex DNA with the centralized lesion mispair and various amounts of E3Q Fpg (1 – 140 nM) were incubated in a buffer containing 10 mM Tris-HCl, pH 7.4, 10 mM NaCl, 0.1 μg/μl BSA, and 500 μM calf thymus DNA at 25 °C for 15 min. The MPE-Fe(II) solution was freshly prepared by mixing equal volumes of 1 mM MPE and 1 mM $Fe(NH_4)_2(SO_4)_2.6H_2O$ followed by a 1:2 dilution in water. A 1:1 mixture of MPE-Fe(II) solution and 10 mM sodium ascorbate (freshly prepared) were added (1 μL each) to the enzyme/DNA mixtures and then incubated at room temperature for 30 min. The reactions were quenched by adding 10 μL of formamide loading dye and incubated at 90 °C for 3 min. Samples were then electrophoresed using a 15% denaturing acrylamide gel in 1× TBE buffer. Control reactions were also performed in the same way in the absence of E3Q Fpg and/or MPE-Fe(II).

Hydroxyl radical footprinting using Fe(II)-EDTA was performed on the E3Q Fpg complex with the Sp:G duplex in a manner analogous to that for MPE-Fe(II), except that 3 μL of a freshly prepared chilled solution containing 0.1% H_2O_2, sodium ascorbate (6.7 mM) and 0.1 mM $[Fe(EDTA)]^{2-}$ [0.2 mM $(NH_4)_2Fe(SO_4)_2$.6H2O and 0.4 mM EDTA] was added to each reaction, instead of the MPE-Fe(II) solution.

Results

EcFpg exhibits high affinity for Gh- and Sp-containing duplexes

Measurements of dissociation constants (K_ds) using electrophoretic mobility shift assays (EMSA) of wild type (WT) EcFpg with substrates and abasic site product analogues have been reported previously (51–55). However, the reported K_d values with the substrates (52–54) are likely actually reporting on K_d values of EcFpg to the product produced during the incubation of the enzyme with the substrate duplex prior to loading onto the gel. In fact, under appropriate K_d conditions, we observed significant amounts of conversion of the DNA substrate (e.g. Gh:C-containing duplex) to product at all concentrations of the enzyme titration (data not shown). Thus, in order to evaluate recognition features of the hydantoin lesion substrates relative to OG without complications associated with the base cleavage reaction, a glycosylase inactive variant, E3Q EcFpg (44), was used. The EMSA experiments were performed using a 30 bp duplex ([DNA] $\ll$ K_d) containing the oxidized lesion (OG, Gh or Sp) base paired with C or G at 25 °C. These two base pairing contexts were chosen since all three lesions are removed efficiently in these contexts. In initial EMSA experiments, we attempted to use 18 bp duplexes containing Gh or Sp. However, with these duplexes as the protein concentration was increased, single-stranded DNA was observed rather than protein-DNA complex suggesting that protein binding destabilizes the 18 bp duplex. Thus, for this reason we turned to using a 30 bp duplex containing the same internal sequence as the 18 bp duplex used previously for kinetic studies. Representative plots of percent protein bound DNA versus E3Q EcFpg concentration from the EMSA experiments are shown in Figure 2, while K_d values determined from at least four different experiments are summarized in Table 1. As expected, E3Q EcFpg exhibits higher affinity for the OG:C duplex (K_d of 280 ± 70 nM) than a non-specific duplex (K_d (est) > 2 μM). However, surprisingly, E3Q EcFpg binds with significantly higher affinity to the Gh and Sp duplexes over the corresponding duplexes containing OG. The apparent dissociation constants observed with the duplex containing Gh:C (0.2 ± 0.1 nM) and Sp:C (0.05 ± 0.01 nM) are 2000-fold and 6000-fold tighter, respectively, than that for the duplex containing the OG:C bp. The binding of E3Q EcFpg is influenced by the base opposite the lesion as evidenced by the K_d values for the Gh:G- and Sp:G-containing duplex of 25 ± 2 nM and 15 ± 2 nM respectively. These values are 200-fold and 400-fold greater than those for the corresponding duplex containing Gh:C and Sp:C, respectively.

Hydroxyl radical footprinting with methidium propyl- EDTA (MPE)-Fe(II)

Fe(II)-EDTA hydroxyl-radical footprinting experiments of EcFpg bound to duplexes containing product analogues, such as THF, have been reported (51,55). In this work, we used MPE-Fe(II) to generate hydroxyl radicals, rather than Fe(II)-EDTA. With the MPEFe(II) reagent, the methidium intercalator delivers the Fe(II)-EDTA moiety to the double helical regions of DNA, and therefore deoxyribose cleavage by the generated hydroxyl radicals occurs more readily in regions of duplex DNA. The 30 bp duplex containing the oxidized lesions (Gh and Sp) paired with either C or G was incubated with increasing amounts of E3Q EcFpg followed by reaction with MPE-Fe(II). In each case, either the lesion-containing strand or the complementary strand had been 5′-end labeled with ^{32}P-containing phosphate to allow for visualization. These strands were also subjected to the G+A Maxam-Gilbert reactions (56) to correlate the footprinted nucleotides surrounding the mispair to the sequence that was used.

Representative storage phosphor autoradiograms of the footprinting experiments with E3Q EcFpg and Sp:C and Gh:C-containing duplexes is shown in Figure 3. As shown in Figure 3, as well as with the analogous duplexes containing Sp:G and Gh:G bps, there is protection due to the presence of E3Q EcFpg on both strands of the DNA duplex. The amount of enzyme required for protection is different in each case, and is consistent with the relevant dissociation constants (K_d) determined for each duplex (Table 1). It is also notable that we have been unable

to observe a defined footprint with the OG:C duplex under our conditions. At concentrations where protection was observed, the entire duplex was protected rather than the just the OG:C bp site. This suggests that a larger difference in affinity, and more importantly enzyme off-rate, for the lesion site and the non-specific duplex may be required to observe a defined region of protection. This result is reminiscent of previous MPE-Fe(II) footprinting experiments with *E. coli* MutY where clear footprinted regions were observed in experiments with duplexes containing OG, but not G, opposite an abasic site or the 2′-deoxyadenosine analogue, 2′-deoxyformycin, despite the fact that MutY is competent at removing adenine when base paired with G and OG (50).

Representative histograms of the regions of the 30 bp DNA duplex surrounding the Gh and Sp opposite C or G protected by E3Q Fpg determined by quantitative analysis of the relevant storage phosphor autoradiograms are shown in Figures 4 and 5, respectively. The trends observed in each of the histograms are similar and the protected region spans 15–16 nts on both strands of the DNA duplex. The footprinting experiments also reveal different patterns of protection of the duplexes containing Gh versus Sp provided by EcFpg with the MPE-Fe (II) footprinting reagent. However, the most striking difference between the results with the Gh and Sp containing duplexes is the hyperreactivity of the Sp nucleotide to cleavage by MPE-Fe(II) generated hydroxyl radicals in the presence of E3Q EcFpg (Figure 3A). The intensity of the cleavage observed at the Sp nt when paired with both G and C was increased approximately 4-fold in the presence of E3Q Fpg over the control with no enzyme.

In order to determine if the hyperreactivity of the Sp nt was related to the presence of the methidium intercalator, hydroxyl radical footprinting using Fe(II)-EDTA of E3Q EcFpg bound to an Sp:G-containing duplex was performed. At the concentration of E3Q EcFpg used in the MPE-Fe(II) footprinting experiments (Figure 3), the intensity of the overall footprint is diminished due to the higher amounts of reagent needed to observe DNA cleavage and the higher accessibility of the footprinting reagent. However, most notably, hyperreactivity of the Sp nt is not observed under these conditions. A marginally increased amount of cleavage of the Sp nt (1.3-fold increased over the control with no protein) was observed when the amount of E3Q Fpg was quite high (100 nM). The extent of the footprinted region with Fe(II)-EDTA was also reduced compared to the Fe-EDTA reagent tethered to methidium (Figure 6). The more efficient cleavage of the Sp nt with MPE-Fe(II) suggests that an intercalation site is created upon binding of E3Q EcFpg to the Sp-containing duplex. However, since some hyperreactivity is observed at high EcFpg concentrations, the presence of EcFpg likely also distorts the Sp nt or alters its accessibility to increase its reactivity with hydroxyl radicals.

Fpg catalyzes the removal of Gh and Sp as efficiently as OG

Under single-turnover conditions (STO) where [DNA] < [Enzyme], we previously established that EcFpg excises OG, Gh and Sp opposite all the four bases in the 18 bp duplex (49). To allow for comparison with the binding and footprinting experiments herein, the kinetic properties with the 30 bp substrates containing Gh, Sp and OG opposite all four natural bases were examined. In each case, the lesion-containing strand was endlabeled with ^{32}P-containing phosphate at the 5′-end, and the activity was assessed by the extent of strand scission at the lesion site as a function of time. EcFpg has previously been shown to catalyze both removal of OG and associated β- and δ-elimination reactions to provide strand scission at the lesion site (57). Importantly, quenching with NaOH gave similar observed rates for strand scission as those that had not been treated with base indicating that intact abasic sites are not present in the reaction under these conditions. This is consistent with tight-association of the glycosylase and lyase functions of EcFpg. Using the kinetic approach and analysis reported previously (49), the rate constant k_2, encompassing all steps involving base excision (Scheme I) were determined. It should be noted that a NaCl concentration of 30 mM was used in these

experiments, however rate constants for several substrates (Sp:G, OG:C, OG:A) were also measured at 100 mM NaCl and similar results were obtained.

Under STO conditions, with the 30 bp duplex at 37 °C, both Gh and Sp are excised opposite all the four bases. The rate of excision of both Gh and Sp are similar to each other, however, the rate constants are much higher when compared to the corresponding rates with the 18 bp duplex (49). The net result is that in the 30 bp duplex sequence, the rate constants for EcFpg catalyzed removal of Gh and Sp opposite C, G and T are similar to those for removal of OG (Table 2). This is in contrast to a reduced rate of removal of Gh and Sp relative to OG in the corresponding 18 bp duplexes when paired with C, T or G reported previously (45). For example, EcFpg catalyzed removal of both Gh and Sp opposite C in the 30 bp duplex provided rate constants of 21 ± 1 min^{-1}, a value that is similar to 16 ± 2 min^{-1} observed for OG removal from the corresponding OG:C-containing duplex. Notably, the rate of OG removal by EcFpg, opposite G, C and T, does not seem to be as sensitive to the duplex length,[3] as is the case with the Gh and Sp. The rates of excision of Gh from Gh:A (1.4 ± 0.2 min^{-1}) and Sp from Sp:A (1.5 ± 0.2 min^{-1}) in the 30 bp duplex are 5-fold higher than that observed for OG excision from OG:A (0.27 ± 0.01 min^{-1}). However, the magnitude of the difference between Gh/Sp and OG in the longer duplex, when paired with A, is slightly smaller than with the 18-bp duplex since OG removal opposite A is enhanced. The trend of preferred removal of Gh and Sp opposite C over A is also maintained. The increased efficiency of removal of Gh and Sp in the longer duplex sequence also results in a slightly increased rate of removal of both lesions opposite C relative to opposite G. Somewhat surprisingly, however, is that even in the longer duplex, the processing of Gh relative to Sp by EcFpg is remarkably similar despite the major differences in the structures of the two hydantoins.

Discussion

Though seemingly deceptively simple, the excision of damaged bases mediated by BER glycosylases is a complex and multi-step process (58,59). Indeed, minimally this process requires initial recognition of the damaged base within duplex DNA, melting of the bp, extrusion of the damaged nucleotide from the helix and stabilization of the appropriate extrahelical conformation for base cleavage (58). In the case of EcFpg, pre-steady state kinetics studies suggest that several transient enzyme substrate complexes must be formed prior to excision of the damaged base (60,61). The lesion-recognition complex (LRC) formed prior to base excision is represented by the structure of E3Q BsFpg bound to an OG:C substrate (Figure 1B) (44). In the LRC, the extrahelical OG is lodged in the *syn* conformation in a large enzyme pocket. Though there are many OG contacts, the main feature not possible with G is a specific hydrogen bond with the carbonyl oxygen of Ser 220 of BsFpg with NH7 of OG. In addition, an important feature of the OG LRC (44), compared to other structures (62,63), was the closure and ordering of a flexible loop around the OG to provide several interactions of backbone amides with the O6 of OG (44). Due to the structural similarities of hydantoins, Gh and Sp to OG, a similar recognition strategy by Fpg enzymes could be envisioned for these lesions (Figure 1). However, some caution should be exercised in making such extensions since structural studies of *Lactococcus lactis* Fpg bound to carbocyclic FapydG-containing DNA revealed a significantly different recognition mode than that observed with OG even though FapydG is quite similar to OG (64). The flexibility to adopt alternate recognition complexes may be a feature that allows Fpg to recognize a wide variety of substrates.

In order to reveal features of recognition and binding unique to the hydantoin lesions separately from base excision, EMSA and footprinting experiments with the inactive variant, E3Q EcFpg

[3]For reference the relevant rate constants (k_2) for OG removal from OG:X-containing 18-bp duplex under the same experimental conditions are as follows: OG:C, 16 ± 2 min^{-1}; OG:T, 16 ± 1 min^{-1}, OG:G, 18 ± 1 min^{-1}, OG:A, 0.05 ± 0.01 min^{-1}.

and duplexes containing Gh, Sp and OG opposite both C and G were performed. An unexpected finding in the EMSA experiments with E3Q EcFpg binding to various lesion-containing duplexes was the higher affinity for the Gh and Sp-containing duplexes over those containing OG. Indeed, E3Q EcFpg exhibits at least three orders of magnitude higher affinity to the Gh and Sp-containing duplexes relative to the corresponding OG-containing duplex. The higher affinity of E3Q EcFpg for the Gh/Sp duplexes may be related to the fact that Gh and Sp lesions are more destabilizing to the DNA duplex than OG as indicated by UV-melting studies (29). The exact amount of destabilization caused by Gh and Sp relative to OG is highly dependent on the sequence and base pairing context, but generally the observed T_m is reduced several degrees with both Gh and Sp. Molecular dynamics simulations also suggested that Sp would cause duplex distortion by affecting base-stacking of the neighboring Watson-Crick bps (65). The reduced local stability of the duplex proximal to the Gh and Sp lesion sites may facilitate opening of the helix and disruption of the base pair. Reduced duplex stability caused by the presence of Gh and Sp-containing bps may be further magnified upon binding of EcFpg. Recent structures of BsFpg forced to interrogate normal non-lesion containing DNA via disulfide-trapping suggest that Fpg actively tests the robustness of bps as part of the search process for DNA damage (66). In these structures, a phenylalanine residue (Phe 144) was found to intercalate at normal bps (G:C, A:T) which resulted in severe buckling of the bp. Though buckled, the Watson-Crick bps remained intact, however, lesion-containing bps may more readily snap open when subjected to these conditions. Once extruded, favorable interactions of the extruded base and the base opposite facilitate capture and excision of the damaged base. If similar hydrogen-bonding interactions in the base-clipping pocket can be made with both OG and the hydantoin lesions, the more facile bp disruption may make the overall affinity higher with the hydantoin lesion duplexes.

The substitution of Glu-3 with Gln in E3Q EcFpg that was made to inactivate the enzyme may also magnify the difference in binding between OG and the Gh and Sp lesion containing duplexes. Glu-3 is located near the N-terminal proline (Pro-2) which is tucked into the active site to participate in the base displacement reaction (57). In the LRC structure, some small differences were observed at position 3 compared to WT BsFpg to avoid steric clashes caused by the presence of the amide –NH2 of Gln-3 (44). In fact, the amide functionality of Gln-3 was observed in the LRC to hydrogen-bond to the 8-oxo-group of OG.

The binding data with E3Q EcFpg also shows tighter binding with duplexes containing Sp opposite both C and G, than the corresponding duplexes containing Gh. This may reflect both more facile disruption of Sp-containing bps and more favorable interactions of Sp within the active site of E3Q EcFpg. Based on its structure, Gh is likely more readily accommodated within the duplex and results in less local bp distortion. If the Gh lesion adopts an enol tautomer this provides a planar base heterocycle that would be even less disruptive to base stacking. In addition, the Gh lesion is positively charged and this feature may provide for favorable interactions with the negatively charged DNA backbone.

The base opposite Gh and Sp also exerts a strong influence on the relative dissociation constants of E3Q EcFpg. The K_d values show that E3Q EcFpg binds more efficiently (200–400 fold) to the hydantoin lesions when paired with C over G. This may be expected since Fpg has been shown to prefer a pyrimidine opposite OG (54). In the structures of Fpg bound to DNA, there is an Arg that fills the void left after extrusion of OG and makes specific hydrogen-bonds to C (44,62,63). The opposite base effect may also be a consequence of more stable base pairing of Gh and Sp with G over C, such that the Gh/Sp:C bp is more easily disrupted and more readily recognized (29). In fact both Gh and Sp can mimic “T” and thus Gh_{syn} or Sp_{syn} can base pair with G in the same fashion as a T_{anti}:G_{anti} wobble pair (Figure 7)(67).

The high affinity of E3Q EcFpg for the Gh and Sp containing duplexes suggested that footprinting techniques would provide insight into the recognition features used by EcFpg with these unique lesions within the DNA. Indeed, footprinting using hydroxyl radicals produced from MPE-Fe(II) revealed that E3Q EcFpg provides an unusual pattern of protected nucleotides. The protected region is extensive encompassing 15–16 nts and spans both the strands of the duplex. This is in contrast to previous results with WT EcFpg bound to a product analogue duplex using Fe-EDTA hydroxyl radical footprinting where protection of a 5–6 nucleotide span on the THF-containing strand was observed (51,55). The footprinting results with MPE-Fe(II) of E3Q Fpg and the hydantoin-containing duplexes also indicate a binding site that is approximately twice as large as what would be anticipated based on the reported Fpg-DNA structures (44,62,63). The larger than expected footprint is due in part to the use of an intercalating footprinting reagent, as is illustrated by the smaller footprint using the Fe(II)-EDTA reagent (Figure 6). The methidium moiety of the MPE-Fe(II) reagent will be unable to intercalate if the protein disrupts the duplex structure or is only contacting one strand of the duplex. Moreover, duplex regions adjacent to the site bound by E3Q EcFpg may be less able to open and unwind to accommodate methidium intercalation. The large footprint is also reflecting on the unusual structural properties of the complex formed between E3Q EcFpg and the duplexes containing the Gh and Sp lesions. Indeed, these results indicate that the structural features of these complexes are distinctly different than the corresponding complexes of Fpg with OG- and abasic site product or analogue-containing duplexes.

The most surprising result from the MPE-Fe(II) footprinting experiments was the observation that while the Gh nt is protected from cleavage by E3Q EcFpg, the binding of E3Q EcFpg to the Sp-containing duplexes makes the Sp nt hyperreactive to hydroxyl radical cleavage. Since MPE-Fe(II) contains an intercalating moiety, delivery of hydroxyl radicals to the vicinity of the Sp sugar likely requires the ability to intercalate at this site. This suggests that in the presence of Fpg, an intercalation site at the Sp nt is created that can accommodate the methidium intercalator. Notably, intercalators often target sites that are more open or deformable, such as mismatched sites in DNA (68) or bulged and triplebase pair sites within RNA (69,70). The unusual spirocyclic structure of Sp may require that the helix be more open at this site; indeed, calculations suggest that in the Sp_{syn} conformation the steric bulk of Sp preferentially shifts the hydantoin ring to the major groove while making hydrogen bonds to G. The shift toward the exterior of the helix leads to less destabilization as a result of the Sp spirocycle (65,71). Moreover, upon binding of E3Q Fpg, the region at the Sp-containing bp may be further altered to create an open base pair platform for the methidium intercalator. Indeed, this is an unusual example of an intercalation site created by the binding of the DNA by a protein. This result is reminiscent of studies with TATA-binding protein (TBP) binding to TATA-sequence containing DNA which created a hot-spot for intercalation and alkylation by the antibiotic pluramycin downstream of the TATA box (72). In this case, it was proposed that the binding of TBP to the TATA box caused transient unwinding on the 3′ side of the binding site that facilitated intercalation; moreover, the intercalation event stabilized the distorted DNA to provide for improved stability of the TBP-TATA complex. The specific recognition of the E3Q EcFpg/Sp-containing DNA duplex complex by MPE-Fe(II) also suggests a unique approach by which such protein/DNA complexes may be targeted by small molecules.

Though the binding studies indicate considerably more affinity of EcFpg for duplexes containing Gh and Sp over OG, the rates of base removal under single-turnover are similar for all three lesions in the 30 bp duplex, when paired opposite C, G or T. This may be due to specific interactions in the base recognition pocket that may be optimized to catalyze removal of OG. In the X-ray structure of the OG LRC (Figure 1), the ordering of the flexible loop (βF-α10) provides for a number of hydrogen-bonding interactions of backbone amides with the O6 of OG (44). These interactions were suggested to be important for stabilizing anion development at O6 of OG as the base is excised from the sugar. Though Gh and Sp may be

accommodated within the base binding pocket, these damaged nucleotides may not be able to achieve the optimal catalytic conformation as readily as OG. Interestingly a recent structure of a mutant of hOGG1 engineered to partially obstruct the active site (Q315F hOGG1) in a complex with an OG:C duplex illustrated that despite the ability to place the OG base nearly completely into the active site, the mutant enzyme cannot catalyze OG excision (73). This suggests that another level of quality control used by BER glycosylases is perfect geometric alignment of the damaged nucleotide within the active site to achieve the optimal transition state for base cleavage. Additional pre-steady state kinetics and structural studies of hydantoin lesions with Fpg and other glycosylases would be exceedingly valuable in further testing these hypotheses.

An important next step will be to determine how the unique features of recognition and removal of the hydantoin lesions by repair enzymes impacts their mutagenic potential in cells. For example, the high affinity of Fpg for the hydantoin lesions *may* translate into more efficient location and excision in a cellular context than OG. Capture of Gh and Sp lesions by repair enzymes prior to replication would be expected to prevent mutagenesis. However, the high miscoding properties of Gh and Sp lesions may be further exacerbated by attempts to repair these lesions in the inappropriate base pairing context. Specifically, the presence of G→C transversion mutations is consistent with the transient formation of Gh:G and Sp:G pairs (34). Removal of the lesion from a Gh:G or a Sp:G bp would enhance mutagenesis mediated by these lesions. Removal of all lesions (OG, Gh, and Sp) opposite A is significantly less efficient than opposite any of the other bases, consistent with a recognition feature that selects against A (45,49). However, EcFpg removes the hydantoin lesions Gh and Sp *more efficiently* than OG when in a base pairing context with A. In the case of OG, removal of misincorporated adenines is performed by *E. coli* MutY; however, the MutY glycosylase does not remove adenine from Gh:A or Sp:A bps to an appreciable extent (49). Recently, the presence of MutY was shown to reduce the bypass efficiency of Gh and Sp-lesions *in vivo* suggesting that MutY may intercept Gh/Sp:A bps and prevent their propagation, thereby mitigating some of their genotoxic properties (35). Thus, clearly lesion recognition and repair are important modifiers of the mutagenesis and toxicity of hydantoin lesions. Further work evaluating the mutagenic potential of Gh and Sp in cellular assays with different repair capabilities may provide interesting connections between properties of these lesions and specific steps in the repair process, as well as further elaborate how these unique lesions contribute to oxidative stress mediated mutagenesis.

Acknowledgements

The pKK-Fapy2 plasmid used for overexpression of WT EcFpg was provided by Dr. Mark Michaels and Dr. Jeffrey Miller (UCLA). We thank Dr. Micheal Leipold for making the plasmid vector pKKE3Q for overexpression of E3Q Fpg. ESI-MS was supported in part by the NSF (CHE-9798413). DNA sequencing was performed by the sequencing facility in the University of Utah Medical School, which is supported in part by an NIH (NCI) grant (5P30CA43014).

References

1. Henle ES, Linn S. Formation, prevention and repair of DNA damage by iron/hydrogen peroxide. J Biol Chem 1997;272:19095–19098. [PubMed: 9235895]
2. Frenkel K. Carcinogen-Mediated Oxidant Formation and Oxidative DNA Damage. Pharmac Ther 1992;53:127–166.
3. Bjelland S, Seeberg E. Mutagenicity, toxicity and repair of DNA base damage induced by oxidation. Mutat Res 2003;531:37–80. [PubMed: 14637246]
4. Beckman KB, Ames BN. Oxidative decay of DNA. J Biol Chem 1997;272:19633–19636. [PubMed: 9289489]
5. Kamiya H. Mutagenic potentials of damaged nucleic acids produced by reactive oxygen/nitrogen species: approaches using synthetic oligonucleotides and nucleotides. Nuc Acids Res 2003;31:517–531.

6. Lindahl T, Wood RD. Quality control by DNA repair. Science 1999;286:1897–1905. [PubMed: 10583946]
7. Friedberg, EC.; Walker, GC.; Seide, W. DNA Repair and Mutagenesis. ASM Press; Washington, DC: 1995.
8. Schärer OD. Chemistry and Biology of DNA Repair. Angew Chemie Int Ed 2003;42:2946–2974.
9. Barnes DE, Lindahl T. Repair and Genetic Consequences of endogenous DNA base damage in mammalian cells. Annu Rev Genet 2004;38:445–476. [PubMed: 15568983]
10. Al-Tassan N, Chmiel NH, Maynard J, Fleming N, Livingston AL, Williams GT, Hodges AK, Davies DR, David SS, Sampson JR, Cheadle JP. Inherited variants of MYH associated with somatic G:C to T:A mutations in colorectal tumors. Nat Genet 2002;30:227–232. [PubMed: 11818965]
11. Ames BN, Shigenaga MK, Hagen TM. Oxidants, antioxidants, and the degenerative diseases of aging. Proc Natl Acad Sci USA 1993;90:7915–7922. [PubMed: 8367443]
12. Ames BN, Gold LS. Endogenous mutagens and the causes of aging and cancer. Mutat Res 1991;250:121.
13. Hoeijmakers JHJ. Genome maintanence mechanisms for preventing cancer. Nature 2001;411:366–374. [PubMed: 11357144]
14. Lindahl T. Instability and decay of the primary structure of DNA. Nature 1993;362
15. Cadet J, Delatour T, T D, Gasparutto D, Pouget JP, Ravanat JL, Sauvaigo S. Hydroxyl radicals and DNA damage. Mutation Research 1999;424:9–21. [PubMed: 10064846]
16. Neeley WL, Essigmann JM. Mechanisms of formation, genotoxicity, and mutation of guanine oxidation products. Chem Res Toxicol 2006;19:491–505. [PubMed: 16608160]
17. Luo W, Muller JG, Rachlin EM, Burrows CJ. Characterization of spiroiminodihydantoin as a product of one-electron oxidation of 8-Oxo-7,8- dihydroguanosine. Org Lett 2000;2:613–616. [PubMed: 10814391]
18. Luo W, Muller JG, Rachlin EM, Burrows CJ. Characterization of hydantoin products from one-electron oxidation of 8-Oxo-7,8-dihydroguanosine in a nucleoside model. Chem Res Toxicol 2001;14:927–938. [PubMed: 11453741]
19. Ye Y, Muller JG, Luo W, Mayne CL, Shallop AJ, Jones RA, Burrows CJ. Formation of 13C, 15N, 18O-labeled guanidinohydantoin from guanosine oxidation with singlet oxygen. Implications in structure and mechanism. J Am Chem Soc 2003;125:13926–13927. [PubMed: 14611206]
20. Ravanat JL, Saint-Pierre C, Di Mascio P, Martinez GR, Medeiros MHG, Cadet J. Damage of isolated DNA mediated by singlet oxygen. Helv Chim Acta 2001;84:13926–13927.
21. Luo W, Muller JG, Burrows CJ. The pH-dependent role of superoxide in riboflavin-catalyzed photooxidation of 8-oxo-7,8-dihydroguanosine. Org Lett 2001;3:2801–2804. [PubMed: 11529760]
22. Misiaszek R, Crean C, Joffe A, Geacintov NE, Shafirovich V. Oxidative DNA Damage associated with combination of guanine and superoxide radicals and repair mechanisms via radical trapping. J Biol Chem 2004;279:32106–32115. [PubMed: 15152004]
23. Sugden KD, Campco CK, Martin BD. Direct Oxidation of guanine and 7,8-dihydro-8-oxoguanosine in DNA by high-valent chromium complex: A possible mechanism for chromate genotoxicity. Chem Res Toxicol 2001;14:1315–22. [PubMed: 11559048]
24. Slade PG, Hailer MK, Martin BD, Sugden KD. Guaninespecific oxidation of double stranded DNA by Cr(VI) and ascorbic acid forms spiroiminodihydantoin and 8-oxo-2′deoxyguanosine. Chem Res Toxicol 2005;18:1140–1149. [PubMed: 16022506]
25. Niles JC, Burney S, Singh SP, Wishnok JS, Tannenbaum SR. Peroxynitrite reaction products of 3′, 5′-di-O-acetyl-8-oxo-7,8-dihydro-2′-deoxyguanosine. Proc Natl Acad Sci 1999;96:11729–11734. [PubMed: 10518518]
26. Niles JC, Wishnok JS, Tannenbaum SR. Spiroiminodihydantoin is the major product of the 8-Oxo-7,8-dihydroguanosine reaction with peroxynitrite in the presence of thiols and guanosine photooxidation by methylene blue. Org Lett 2001;3:963–966. [PubMed: 11277770]
27. Niles JC, Wishnok JS, Tannenbaum SR. Spiroiminodihydantoin and guanidinohydantoin are the dominant products of 8-oxoguanosine oxidation at low fluxes of peroxynitrite: mechanistic studies with 18O. Chem Res Toxicol 2004;17:1510–1519. [PubMed: 15540949]

28. Hailer MK, Slade PG, Martin BD, Sugden KD. Nei deficient Escherichia coli are sensitive to chromate and accumulate the oxidized guanine lesion spiroiminodihydantoin. Chem Res Toxicol 2005;18:1378–1383. [PubMed: 16167829]
29. Kornyushyna O, Berges AM, Muller JG, Burrows CJ. In vitro nucleotide misinsertion opposite the oxidized guanosine lesions spiroiminodihydantoin and guanidinohydantoin and DNA synthesis past the lesions using *Escherichia coli* DNA polymerase I (Klenow fragment). Biochemistry 2002;41:15304–15314. [PubMed: 12484769]
30. Kornyushyna O, Burrows CJ. Effect of the oxidized lesions spiroiminodihydantoin and guanidinohydantoin on proofreading by *Escherichia coli* DNA polymerase I (Klenow Fragment) in different sequence contexts. Biochemistry 2003;42:13008–13018. [PubMed: 14596616]
31. Shibutani S, Takeshita M, Grollman AP. Insertion of specific bases during DNA synthesis past the oxidtion-damaged base 8-oxodG. Nature 1991;349:431–434. [PubMed: 1992344]
32. Grollmann AP, Moriya M. Mutagenesis by 8-oxoguanine: an enemy within. Trends Genet 1993;9:246–249. [PubMed: 8379000]
33. Wood ML, Esteve A, Morningstar ML, Kuziemko GM, Essigmann JM. Genetic effects of oxidative DNA damage: comparative mutagenesis of 7,8-dihydro-8-oxoguanine and 7,8-dihydro-8-oxoadenine in Escherichia coli. Nucleic Acids Res 1992;20:6023–6032. [PubMed: 1461734]
34. Henderson PT, Delaney JC, Muller JG, Neeley WL, Tannenbaum SR, Burrows CJ, Essigmann JM. The hydantoin lesions from oxidation of 7,8-dihydro-8-oxoguanine are potent sources of replication errors in vivo. Biochemistry 2003;42:9257–9262. [PubMed: 12899611]
35. Delaney S, Neeley WL, Delaney JC, Essigman JM. The Substrate Specificity of MutY for Hyperoxidized Guanine Lesions in Vivo. Biochemistry 2007;46:1448–1455. [PubMed: 17260974]
36. Michaels ML, Cruz C, Grollman AP, Miller JH. Evidence that MutY and MutM combine to prevent mutations by an oxidatively damaged form of guanine in DNA. Proc Natl Acad Sci 1992;89:7022–7025. [PubMed: 1495996]
37. Michaels ML, Tchou J, Grollman AP, Miller JH. A repair system for 8-oxo-7,8-dihydroguanine. Biochemistry 1992;31:10964–10968. [PubMed: 1445834]
38. Tajiri T, Maki H, Sekiguchi M. Functional cooperation of MutT, MutM and MutY proteins in preventing mutations casued by spontaneous oxidation of guanine nucleotide in *Escherichia coli*. Mutat Res 1995;336:257–267. [PubMed: 7739614]
39. Krokan HE, Standal R, Slupphaug G. DNA glycosylases in the base excision repair of DNA. Biochem J 1997;325:1–16. [PubMed: 9224623]
40. David SS, Williams SD. Chemistry of glycosylases and endonucleases involved in base-excision repair. Chem Rev 1998;98:1221–1261. [PubMed: 11848931]
41. Parikh SS, Mol CD, Tainer JA. Base excision repair family portrait:integrating the structure and chemistry of an entire DNA repair pathway. Structure 1997;5:1543–1550. [PubMed: 9438868]
42. Fromme JC, Banerjee A, Verdine GL. DNA glycosylase recognition and catalysis. Curr Opin Struct Biol 2004;14:43–49. [PubMed: 15102448]
43. Fromme JC, Verdine GL. Base Excision Repair. Adv Prot Chem 2004;69:1–41.
44. Fromme CJ, Verdine GL. DNA lesion recognition by the bacterial repair enzyme MutM. J Biol Chem 2003;278:51543–51548. [PubMed: 14525999]
45. Leipold MD, Workman H, Muller JG, Burrows CJ, David SS. Recognition and removal of oxidized guanines in duplex DNA by the base excision repair enzymes hOGG1, yOGG1, and yOGG2. Biochemistry 2003;42:11373–11381. [PubMed: 14503888]
46. Hazra TK, Muller JG, Manuel RC, Burrows CJ, Lloyd RS, Mitra S. Repair of hydantoins, one electron oxidation product of 8-oxoguanine, by DNA glycosylases of *Escherichia coli*. Nucleic Acids Res 2001;29:1967–1974. [PubMed: 11328881]
47. Hailer MK, Slade PG, Martin BD, Rosenquist TA, Sugden KD. Recognition of the oxidized lesions spiroiminodihydantoin and guanidinohydantoin in DNA by the mammalian base excision repair glycosylases NEIL1 and NEIL2. DNA Repair 2005;4:41–50. [PubMed: 15533836]
48. Micheals ML, Pham L, Cruz C, Miller JH. MutM, a protein that prevents G-C to T-A transversions, is foramidopyrmidine-DNA glycosylase. Nucleic Acids Research 1991;19:3629–3632. [PubMed: 1649454]

49. Leipold MD, Muller JG, Burrows CJ, David SS. Removal of hydantoin products of 8-oxoguanine oxidation by the Escherichia coli DNA repair enzyme, Fpg. Biochemistry 2000;39:14984–14992. [PubMed: 11101315]
50. Porello SL, Williams SD, Kuhn H, Michaels ML, David SS. Specific recognition of substrate analogs by the DNA mismatch repair enzyme MutY. J Am Chem Soc 1996;118:10684–10692.
51. Tchou J, Michaels ML, Miller JH, Grollman AP. Function of the Zinc finger in *Escherichia coli* Fpg protein. J Biol Chem 1993;268:26738–26744. [PubMed: 8253809]
52. Tchou J, Bodepudi V, Shibutani S, Antoscheckin I, Miller J, Grollman AP, Johnson FP. Substrate Specificity of Fpg Protein. J Biol Chem 1994;269:15318–15324. [PubMed: 7515054]
53. Zaika EI, Perlow RA, Matz E, Broyde S, Gilboa R, Grollman AP, Zharkov DO. Substrate Discrimination by Formamidopyrimidine-DNA Glycosylase. J Biol Chem 2004;279:4849–4861. [PubMed: 14607836]
54. Castaing B, Geiger A, Seliger H, P N, Laval J, Zelwer C, Boiteux S. Cleavage and binding of a DNA fragment containing a single 8-oxoguanine by wild type and mutant FPG proteins. Nucleic Acids Res 1993;21:2899–2905. [PubMed: 8332499]
55. Castaing B, Fourrey JL, Hervouet N, Thomas M, Boiteux S, Zelwer C. AP site structural determinants for Fpg specific recognition. Nucleic Acids Res 1999;27(2):608–615. [PubMed: 9862987]
56. Maxam AM, Gilbert W. Sequencing end-labeled DNA with base specific chemical cleavages. Methods Enzymol 1980;65:499–560. [PubMed: 6246368]
57. Zharkov DO, Rieger RA, Iden CR, Grollman AP. NH_2-terminal proline acts as a nucleophile in the glycosylase/AP-lyase reaction catalyzed by *Escherichia coli* Formamidopyrimidine-DNA glycosylase (Fpg) protein. J Biol Chem 1997;272:5335–5341. [PubMed: 9030608]
58. Stivers JT. Site-Specific DNA Damage Recognition by Enzyme-Induced Base Flipping. Prog Nucl Acid Res Mol Biol 2004;77:37–65.
59. Hitomi K, Iwai S, Tainer JA. The intricate structural chemistry of base excision repair machinery: Implications for DNA damage recognition, removal and repair. DNA Repair. 2007in press
60. Koval VV, Kuznetsov NA, Zharkov DO, Ishchenko AA, Douglas KT, Nevinsky GA, Federova OS. Pre-steady-state kinetics shows differences in processing of various DNA lesions by Escherichia coli formamidopyrimidine-DNA glycosylase. Nucleic Acids Res 2004;32:926–935. [PubMed: 14769949]
61. Kuznetsov NA, Koval VV, Zharkov DO, Vorobjev YN, Nevinsky GA, Douglas KT, Fedorova OS. Pre-Steady-State Kinetic Study of Substrate Specificity of Escherichia coli Formamidopyrimidine-DNA Glycosylase. Biochemistry 2007;46:424–435. [PubMed: 17209553]
62. Fromme CJ, Verdine GL. Structural insights into lesion recognition and repair by the bacterial 8-oxoguanine DNA glycosylase Mut M. Nature Structural Biology 2002;9:544–552.
63. Gilboa R, Zharkov DO, Golan G, Fernandes AS, Gerchman SE, Matz E, Kycia J, Grollman AP, Shoham G. Structure of formamidopyrimidine-DNA glycosylase covalently complexed to DNA. J Biol Chem 2002;277:19811–19816. [PubMed: 11912217]
64. Coste F, Ober M, Carell T, Boiteux S, Zelwer C, Castaing B. Structural Basis for the Recognition of the FapydG Lesion (2,6-Diamino-4-hydroxy-5-formamidopyrimidine) by Formamidopyrimidine-DNA Glycosylase. J Biol Chem 2004;279:44074–44083. [PubMed: 15249553]
65. Jia L, Shafirovich V, Shapiro R, Geacintov NE, Broyde S. Structural and thermodynamic features of spiroiminodihydantoin damaged DNA duplexes. Biochemistry 2005;44:13342–13353. [PubMed: 16201759]
66. Banerjee A, Santos WL, Verdine GL. Structure of a DNA Glycosylase Searching for Lesions. Science 2006;311:1153–1157. [PubMed: 16497933]
67. Zhao X, Muller JG, Halasyam M, David SS, Burrows CJ. In vitro ligation of oligodeoxynucleotides containing C8-oxidized purine lesions using bacteriophage T4 DNA ligase. Biochemistry 2007;46:3734–3744. [PubMed: 17323928]
68. Junicke H, Hart JR, Kisko J, Giebov O, Kirsch IR, Barton JK. A rhodium (III) complex for high-affinity DNA base-pair mismatch recognition. Proc Natl Acad Sci USA 2003;100:3737–3742. [PubMed: 12610209]
69. Chow CS, Barton JK. Transition Metal complexes as probes of nucleic acids. Methods Enzymol 1992;212:219–242. [PubMed: 1381460]

70. Carlson CB, Vuyisich M, Gooch BD, Beal PA. Preferred RNA binding sites for a threading intercalator revealed by in vitro evolution. Chem Biol 2003;7:663–72. [PubMed: 12890540]

71. Jia L, Shafirovich V, Shapiro R, Geacintov NE, Broyde S. Spiroiminodihydantoin lesions derived from guanine oxidation. Biochemistry 2005;44:6043–6051. [PubMed: 15835893]

72. Sun D, Hurley LH. TBP binding to the TATA box induces a specific downstream unwinding site that is targeted by pluramycin. Chem Biol 1995;2:457–469. [PubMed: 9383448]

73. Radom CT, Banerjee A, Verdine GL. Structural characterization of human 8-oxoguanine DNA glycosylase variants bearing active site mutations. J Biol Chem 2007;282:9182–9194. [PubMed: 17114185]

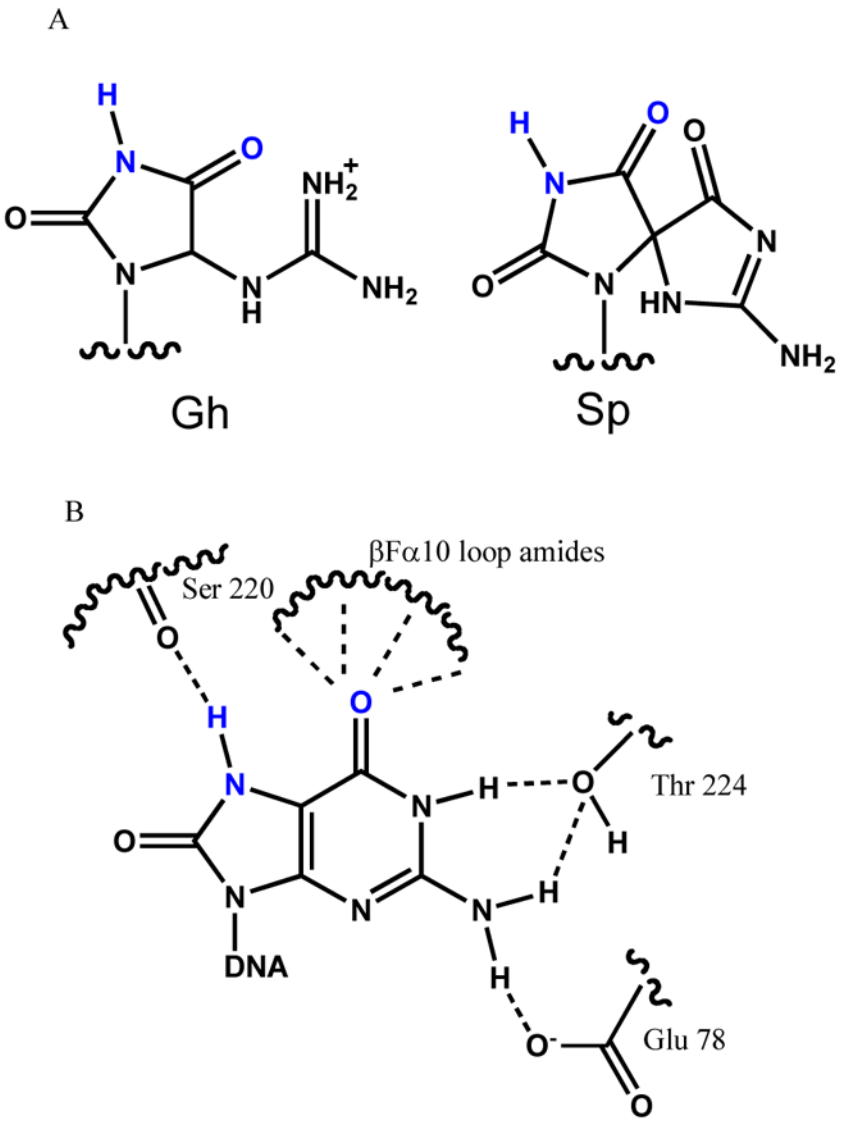

Figure 1. (A) Structures of Guanidinohydantoin (Gh) and Spiroiminodihydantoin (Sp) and (B) Schematic of contacts made to 8-oxoguanine by E3Q BsFpg

(44) (A) The hydantoin products Gh and Sp form from oxidation of OG or G with a variety of oxidants. Atoms that provide structural similarity to OG are colored in blue. (B) Residues and regions of the BsFpg enzyme that are involved in OG-specific contacts are indicated. The βFα10 loop refers to a loop that is ordered only in structures with OG intact (44). There are many backbone amides (of residues 222-225 in βFα10) that are positioned in close proximity to the O6 of OG. Atoms that provide OG specific contacts with BsFpg are shown in blue. Note Fpg makes contacts to C that are not shown.

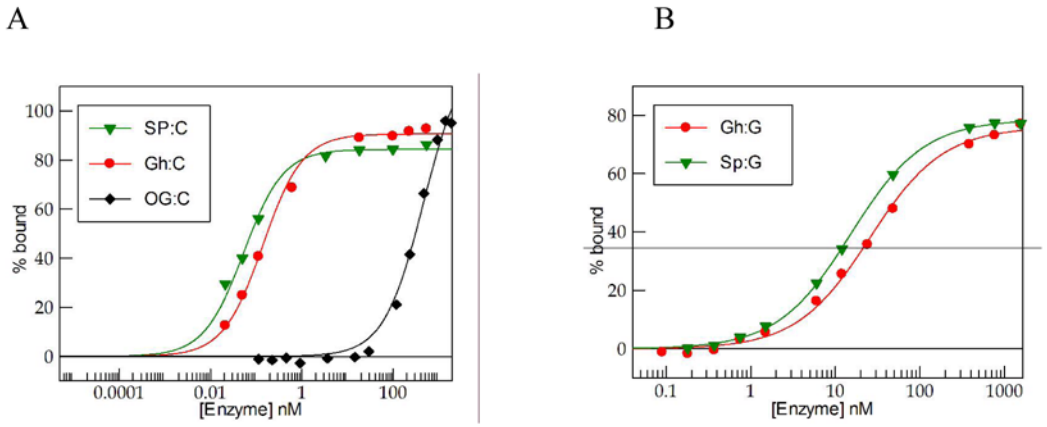

Figure 2. Representative data from EMSA of E3Q Fpg binding to OG-, Gh- and Spcontaining 30-bp duplexes illustrating relative affinity for the different lesions and changes with opposite base

A) Plot of percent E3Q Fpg bound to duplex containing a central OG:C (closed black squares), Gh:C (closed red circles) or Sp:C (closed green triangles) base pairs as a function of E3Q Fpg concentration at 25 °C.

B) Plot of percent E3Q Fpg bound to duplexes containing a central Gh:G (closed red circles) or Sp:G (closed green triangles) DNA as a function of E3Q Fpg concentration at 25 °C.

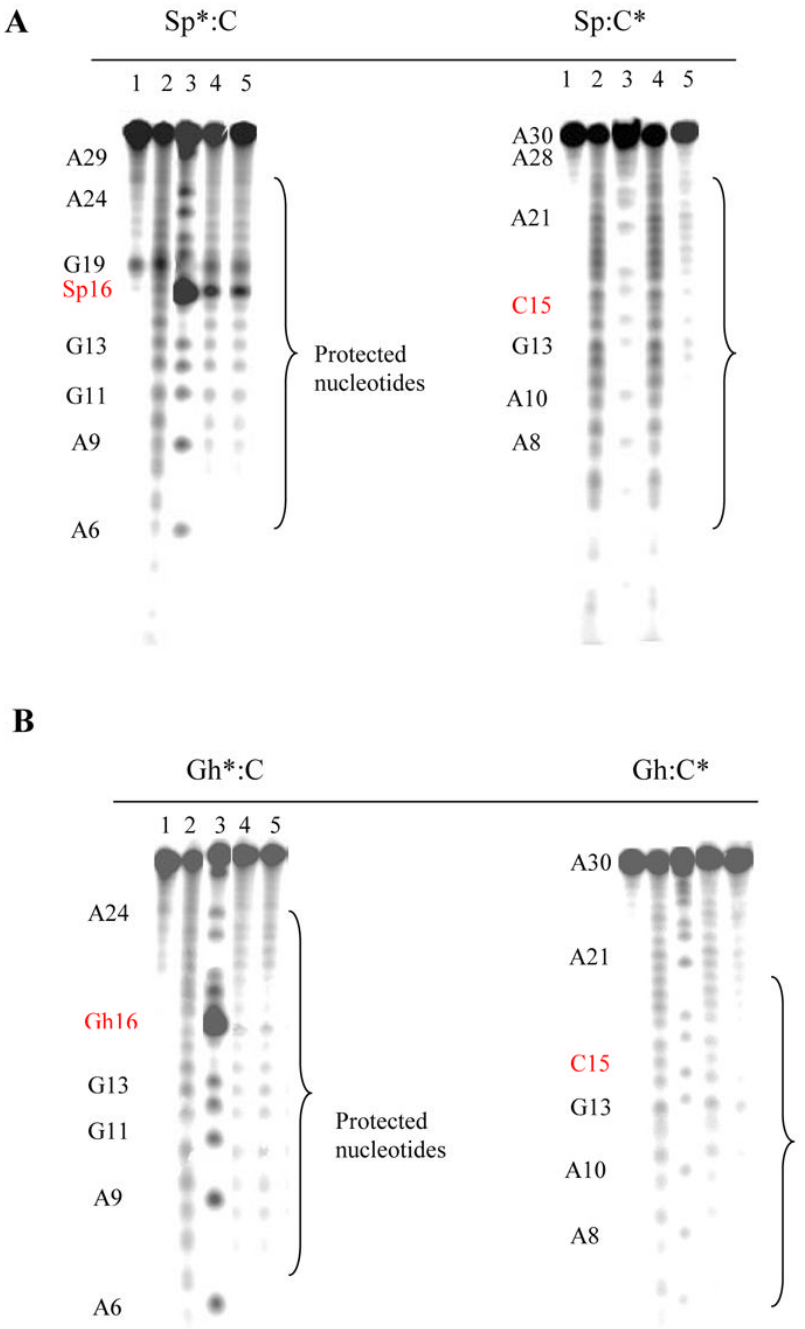

Figure 3. Storage phosphor autoradiogram of hydroxyl radical footprinting using MPE-Fe(II) of E3Q EcFpg with a 30-bp Sp:C and Gh:C duplex

The 30-bp DNA duplex containing the Sp:C mispair (A) or Gh:C mispair (B) was 5′-end labeled either on the Sp/Gh or C-strand. The strand that is labeled in each case is denoted with an asterisk (*). The DNA was incubated at 25 °C in reactions under varying conditions: lane 1, no enzyme and no MPE-Fe(II) control; lane 2, no enzyme control; lane 3, G+A Maxam-Gilbert sequencing; lane 4, 3.5 nM E3Q EcFpg; lane 5, 7 nM E3Q EcFpg. The position of the base pair, Sp:C or Gh:C, is highlighted in red.

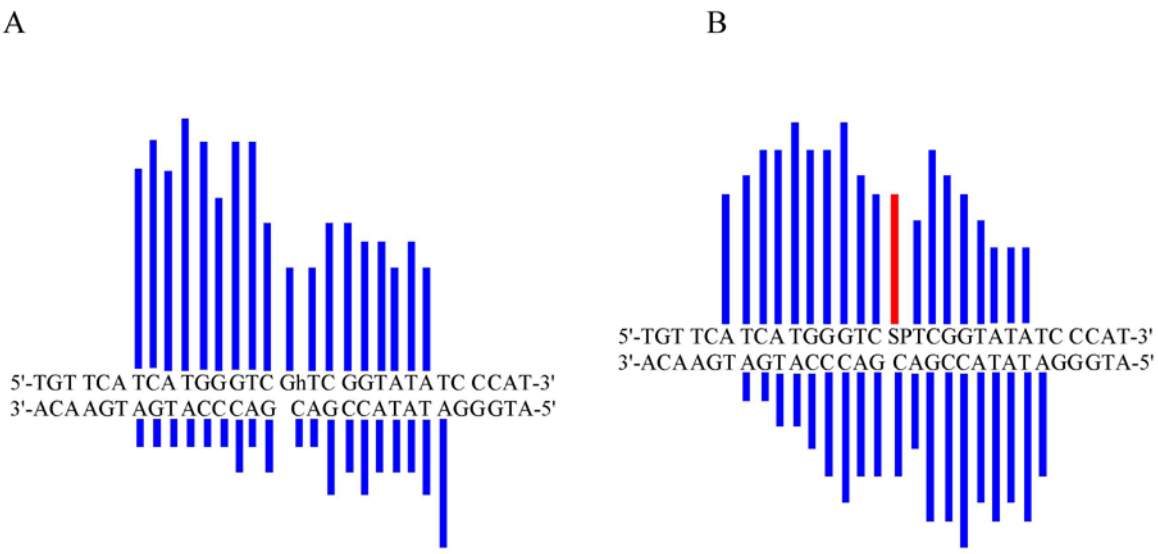

Figure 4. Hydroxyl radical footprinting using MPE-Fe(II) of E3Q EcFpg with Gh:C and Sp:C duplexes

Histogram of the hydroxyl radical footprinting with the 30-bp Gh:C (A) and Sp:C (B) duplexes illustrate the extent of protection from hydroxyl radical footprinting. The data were obtained by quantification of storage phosphor autoradiograms such as the one shown in Figure 3. The blue colored bars represent the footprinted nucleotides while the red bar indicates a hyperreactive site. This histograms for Gh:C and Sp:C were determined from quantitation of the autoradiogram with 7 nM E3Q EcFpg concentration. For these two duplexes, the nucleotide with the maximum protection from the hydroxyl radical cleavage is taken as the standard and denoted by the highest bar. The extent of protection (or hyperreactivity) for the remaining nucleotides is depicted as relative to this standard nucleotide. The absolute intensity of the cleavage at the Sp nucleotide in the presence of E3Q EcFpg is approximately 4-fold increased relative to the control without enzyme.

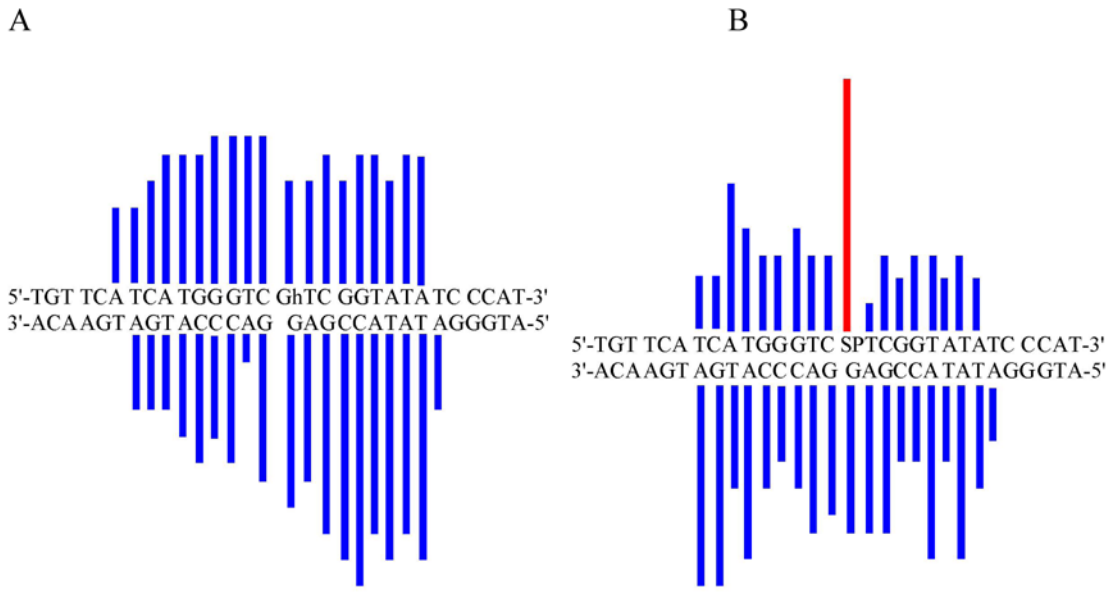

Figure 5. Hydroxyl radical footprinting using MPE-Fe(II) of E3Q EcFpg with Gh:G and Sp:G duplexes

Histograms of the hydroxyl radical footprinting with the 30-bp Gh:G (A) and Sp:G (B) duplexes illustrate the extent of protection from hydroxyl radical footprinting. The data were obtained by quantification of storage phosphor autoradiograms such as the one shown in Figure 3. The blue colored bars represent the footprinted nucleotides while the red bar indicates sites of hyperreactivity. The histogram for the Gh:G and Sp:G is obtained at 70 nM E3Q EcFpg concentration. For these two duplexes, the nucleotide with the maximum protection from the hydroxyl radical cleavage is taken as the standard and denoted by the highest bar. The extent of protection or hyperreactivity for the remaining nucleotides is depicted as relative to this standard nucleotide. The absolute intensity of the cleavage at the Sp nucleotide in the presence of E3Q EcFpg is approximately 4-fold increased relative to the control without enzyme.

Figure 6.
Relative extents of regions of DNA duplex protected by E3Q EcFpg using hydroxyl radical cleavage with Fe-EDTA (dark blue) versus MPE-Fe(II) (red).

A

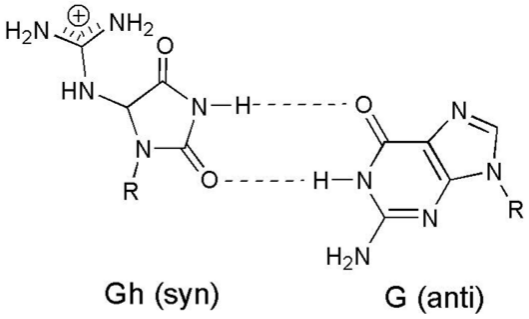

B

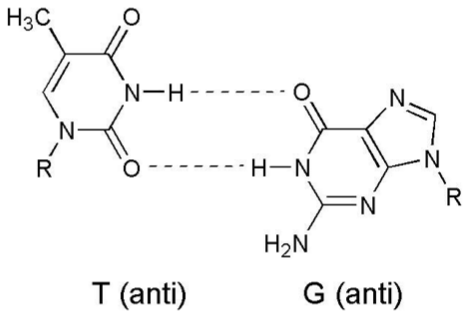

C

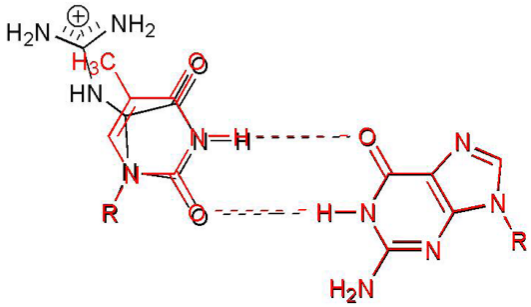

Figure 7. Proposed base pairing of Gh with G

A. Proposed base pairing of Gh_{syn}:G_{anti}

B. Wobble base pairing of T_{anti}:G_{anti}

C. Overlay of the Gh_{syn}:G_{anti} base pair on the T_{anti}:G_{anti} base pair

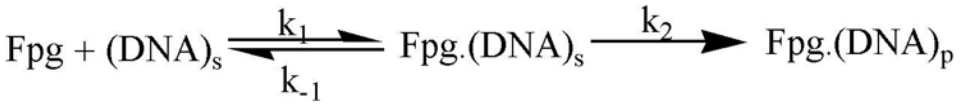

Scheme I.

Table 1

Dissociation constants (K_d[a]) for E3Q EcFpg with the 30-bp duplex at 25 °C

Central bp	E3Q Fpg (nM)
OG:C	280 ± 70
Gh:C	0.2 ± 0.1
Sp:C	0.05 ± 0.02
Gh:G	25 ± 2
Sp:G	15 ± 2

K_d[a]: K_d apparent

Table 2

Rate constants (k_2) determined for the processing of the 30-bp duplex by EcFpg under single-turnover conditions at 37 °C

Central bp	k_2 (min^{-1})	Central bp	k_2 (min^{-1})
OG:C	16 ± 2	OG:G	13 ± 1
Gh:C	21 ± 1	Gh:G	14 ± 1
Sp:C	21 ± 1	Sp:G	15 ± 1
OG:A	0.27 ± 0.01	OG:T	10 ± 1
Gh:A	1.4 ± 0.2	Gh:T	16 ± 1
Sp:A	1.5 ± 0.2	Sp:T	14 ± 1